**NUSANTARA BIOSCIENCE**
Volume 18, Number 1, June 2026
Pages: 17

ISSN: 2087-3948
E-ISSN: 2087-3956
https://doi.org/10.13057/nusbiosci/n180105

# Prediction of potential climate change impacts on the geographic distribution shift of *Selaginella kraussiana* and *S. uncinata* in East, South and Southeast Asia

**AHMAD DWI SETYAWAN[1,2,♥], SUTARNO[3], SUGIYARTO[3], SUNARTO[1], ILYAS NURSAMSI[4], MUHAMMAD NUR SULTON[1], GILANG DWI NUGROHO[3,5,6]**
[1]Department of Environmental Science, Faculty of Mathematics and Natural Sciences, Universitas Sebelas Maret. Jl. Ir. Sutami 36A, Surakarta 57126, Central Java, Indonesia. Tel./fax.: +62-271-663375, ♥email: volatileoils@gmail.com
[2]Biodiversity Research Group, Universitas Sebelas Maret. Jl. Ir. Sutami 36A, Surakarta 57126, Central Java, Indonesia
[3]Department of Biology, Faculty of Mathematics and Natural Sciences, Universitas Sebelas Maret. Jl. Ir. Sutami 36A, Surakarta 57126, Central Java, Indonesia
[4]School of Earth and Environmental Science, Faculty of Science, The University of Queensland. St Lucia 4072, Brisbane, Queensland, Australia
[5]School of Life Sciences and Technology, Institut Teknologi Bandung. Jl. Ganesa No. 10, Bandung 40132, West Java, Indonesia
[6]Biodiversity Study Club, Faculty of Mathematics and Natural Sciences, Universitas Sebelas Maret. Jl. Ir. Sutami 36A, Surakarta 57126, Central Java, Indonesia

Manuscript received: 23 July 2025. Revision accepted: 29 May 2026.

**Abstract.** *Setyawan AD, Sutarno, Sugiyarto, Sunarto, Nursamsi I, Sulton MN, Nugroho GD. 2026. Prediction of potential climate change impacts on the geographic distribution shift of* Selaginella kraussiana *and* S. uncinata *in East, South and Southeast Asia. Nusantara Bioscience 18 (1): n180105. https://doi.org/10.13057/nusbiosci/n180105.* Climate change is increasingly altering the geographic distribution of invasive plant species, yet comparative assessments of closely related invasive taxa remain limited. This study evaluated the potential impacts of climate change on the future distribution of two invasive lycophytes, *Selaginella kraussiana* and *S. uncinata*, across East, South, and Southeast Asia. Species distribution models were developed using the Maximum Entropy (MaxEnt) algorithm based on occurrence records compiled from GBIF, field observations, and published literature. The models incorporated 15 environmental variables representing bioclimatic, edaphic, UVB-radiation, and topographic factors. Future habitat suitability was projected for 2030, 2050, and 2080 under four Representative Concentration Pathway (RCP) scenarios (2.6, 4.5, 6.0, and 8.5). Model performance was high for both species, with AUC values of 0.935 for *S. kraussiana* and 0.966 for *S. uncinata*, indicating excellent predictive accuracy. Environmental controls differed markedly between the species. *Selaginella kraussiana* was primarily associated with temperature-related variables, particularly the minimum temperature of the coldest month (bio_6), whereas *S. uncinata* was more strongly associated with annual precipitation (bio_12) and other moisture-related variables. Future projections indicated substantial habitat expansion for *S. kraussiana*, with total suitable habitat increasing from $11.47 \times 10^6$ km$^2$ under current conditions to $16.43 \times 10^6$ km$^2$ under RCP 8.5 by 2080. Expansion was projected mainly into higher-latitude and higher-elevation subtropical and temperate regions. In contrast, *S. uncinata* exhibited relatively stable distribution patterns, with total suitable habitat changing only slightly from $2.95 \times 10^6$ km$^2$ to $3.04 \times 10^6$ km$^2$ across future climate scenarios. These findings suggest that *S. kraussiana* may experience a greater climate-driven increase in invasion potential than *S. uncinata* and demonstrate the value of integrating species distribution modeling with ecological interpretation to support invasion-risk assessment, early detection, and climate-adaptive management of invasive lycophytes in Asia.

**Keywords:** Climate change, invasive alien species, MaxEnt, *Selaginella kraussiana, Selaginella uncinata*

## INTRODUCTION

Rising global temperatures and shifting precipitation patterns are reshaping the geographic distribution of plant species worldwide, forcing many species to migrate, adapt, or face local extinction (Parmesan and Yohe 2003; Bellard et al. 2012). These changes are particularly concerning in biodiversity hotspots such as East, South, and Southeast Asia, which harbor exceptionally rich endemic flora yet remain highly vulnerable to climate-induced disturbances (Sodhi et al. 2004; Hughes 2017). One of the most important ecological consequences is the accelerated spread of Invasive Alien Species (IAS), which can cause substantial environmental and economic impacts (Pyšek et al. 2020). Climate change may further facilitate biological invasions by creating environmentally suitable conditions in regions that were previously unfavorable for invasive plants (Hellmann et al. 2008). Consequently, understanding how future climate change may alter the potential distribution of invasive species has become increasingly important for effective risk assessment and management.

The genus *Selaginella* (Selaginellaceae) comprises more than 700 species of lycophytes, many of which exhibit remarkable adaptability to diverse environmental conditions (Setyawan 2011). Two species warrant particular attention: *Selaginella kraussiana* and *S. uncinata*. *Selaginella kraussiana*, native to Africa, has successfully invaded Australia, New Zealand, Europe, and the Americas (Dang et al. 2019). This creeping clubmoss thrives in humid environments and has been widely traded as an ornamental plant (Gola and Jernstedt 2016). In New Zealand, it is recognized as a significant invasive weed capable of displacing native ground flora (Nessia et al. 2014). Similarly, *S. uncinata*, native to southern China, has been introduced across Asia as an ornamental ground cover (Setyawan 2014; Qin et al. 2022). Its rapid vegetative growth enables it to colonize new habitats efficiently, potentially threatening indigenous understory vegetation (Li et al. 2021). Despite their recognized invasiveness, the potential future distribution of these two species under climate change scenarios in Asia remains poorly understood.

East, South, and Southeast Asia represent particularly important regions for evaluating the future invasion risk of both species. These regions contain several globally recognized biodiversity hotspots, including Sundaland, Indo-Burma, Wallacea, and the Eastern Himalayas, while simultaneously experiencing rapid urbanization, expanding ornamental horticulture industries, and increasing interregional plant trade (Myers et al. 2000; Hughes 2017). Both *S. kraussiana* and *S. uncinata* are actively cultivated and traded as ornamental plants across many parts of Asia, particularly in humid tropical and subtropical highlands. In addition, documented naturalized populations have already been reported in several Asian regions, including China, Japan, Taiwan, Indonesia, and Vietnam (Setyawan 2014; Dang et al. 2019). These conditions make Asia an important socio-ecological region for assessing potential climate-driven expansion and future invasion risk of introduced *Selaginella* species.

Species Distribution Models (SDMs) are powerful tools for predicting how climate change may alter species' geographic ranges (Elith and Leathwick 2009). Among SDM algorithms, Maximum Entropy (MaxEnt) has become widely adopted because of its robust performance with presence-only data (Phillips et al. 2006; Phillips and Dudík 2008). MaxEnt has been successfully applied to forecast climate-driven range shifts for numerous invasive plants worldwide (West et al. 2016). For *Selaginella* species, previous studies have demonstrated the utility of MaxEnt in predicting distributions in Southeast Asia (Setyawan et al. 2018, 2021). However, no comprehensive comparative study has yet examined how *S. kraussiana* and *S. uncinata* may respond differently to future climate scenarios across East, South, and Southeast Asia.

This study aimed to predict the potential impacts of climate change on the geographic distribution shifts of *S. kraussiana* and *S. uncinata* across East, South, and Southeast Asia. Using the MaxEnt algorithm with a comprehensive set of environmental variables representing bioclimatic, edaphic, UVB radiation, and topographic factors, we modeled current suitable habitats and projected future distribution shifts under four RCP scenarios (2.6, 4.5, 6.0, and 8.5) for 2030, 2050, and 2080. We further identified the principal environmental drivers associated with each species and quantified changes in suitable habitat area across all climate scenarios to compare species-specific responses to future climate change and evaluate the consistency of projected distributional trends through time.

We hypothesized that future climate warming would differentially alter the distribution patterns of *S. kraussiana* and *S. uncinata* across Asia due to contrasting thermal and hydrological constraints. Specifically, *S. kraussiana* was expected to exhibit greater habitat expansion under warming scenarios because reduced thermal limitations may increase climatic suitability and facilitate range expansion into previously unsuitable regions. In contrast, *S. uncinata* was predicted to maintain comparatively stable distributions owing to its stronger association with persistently humid environments and hydrological stability. Accordingly, this study aimed to evaluate species-specific responses to future climate change by quantifying projected changes in habitat suitability, identifying key environmental drivers, and comparing distributional shifts under multiple climate scenarios. The findings are expected to support invasion-risk assessment, early detection, and climate-adaptive management strategies for invasive *Selaginella* species in Asia.

## MATERIALS AND METHODS

### Study area

This study focuses on East, South, and Southeast Asia, a geographically diverse region spanning approximately 21.5 million km² between 26°E-170°E and 11°S-80°N (Figure 1). The region encompasses major biodiversity hotspots including the Eastern Himalayas, Indo-Burma, Sundaland, Wallacea, the Philippines, and East Asian islands (Myers et al. 2000; Sodhi et al. 2004). Climatic conditions range from tropical rainforests in Southeast Asia (mean annual temperature >25°C, precipitation >2,500 mm/yr) to temperate zones in East Asia with distinct seasonal variation, as well as alpine environments in the Himalayan belt (Hughes 2017). Both *S. kraussiana* and *S. uncinata* have been documented across this region through natural dispersal and ornamental trade, with established naturalized populations reported in China, India, Indonesia, Japan, Taiwan, and Vietnam (Setyawan 2014; Dang et al. 2019).

### Species occurrence data

Occurrence records of *S. kraussiana* and *S. uncinata* were compiled from the Global Biodiversity Information Facility (GBIF 2024; www.gbif.org) and supplemented with field observations and published taxonomic and ecological studies of *Selaginella* in Southeast Asia (Setyawan 2011, 2014; Setyawan et al. 2015). To minimize spatial bias and model overfitting, duplicate records and occurrences lacking coordinates or containing invalid, erroneous, or highly uncertain geographic information were excluded (Kramer-Schadt et al. 2016). All records were visually inspected to identify georeferencing errors and occurrences located outside the known distribution range of each species. Spatial thinning was subsequently performed using the *spThin* package in R 4.2.0, applying a minimum distance of 5 km between occurrence points to reduce spatial clustering and autocorrelation (Aiello-Lammens et al. 2015; R Core Team 2022). After data cleaning and thinning, the final dataset comprised 1,592 occurrence records for *S. kraussiana* (1,590 GBIF records and 2 field records) and 470 occurrence records for *S. uncinata* (465 GBIF records and 5 field records). The occurrence data were exported as Comma-Separated Value (CSV) files containing species names and geographic coordinates (longitude and latitude) for subsequent MaxEnt modeling (Phillips et al. 2006). Although these procedures substantially reduced sampling bias, some residual bias may remain because biodiversity records are often concentrated in more accessible or intensively surveyed regions (Kramer-Schadt et al. 2016).

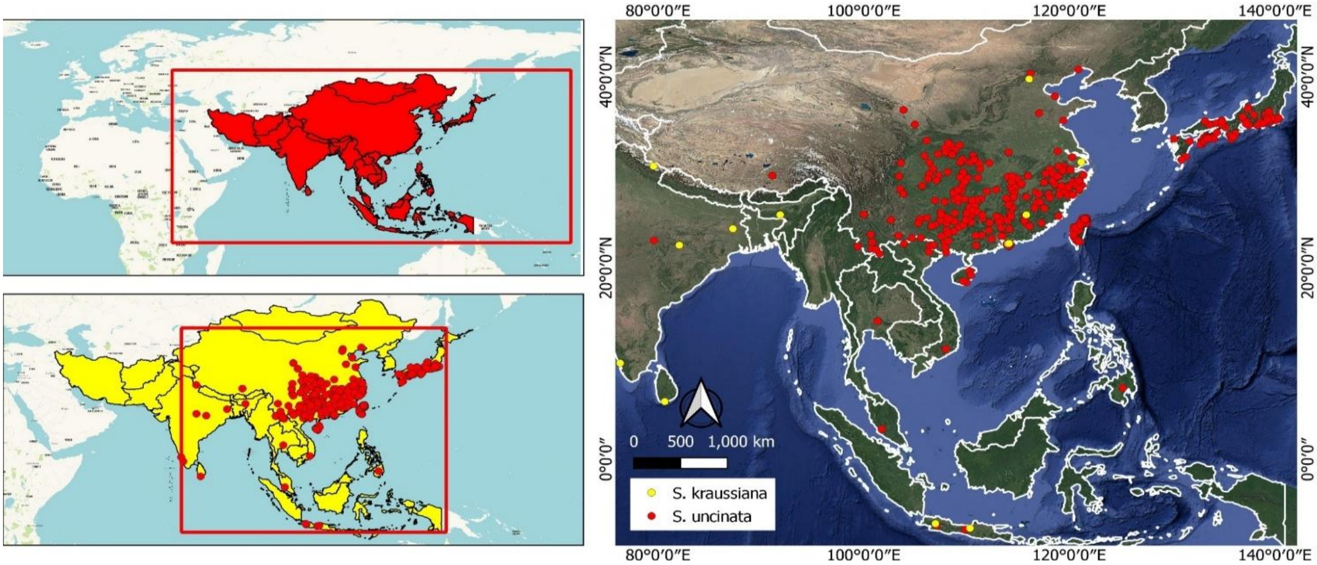

**Figure 1.** Study area and occurrence records of *Selaginella kraussiana* (yellow circles) and *S. uncinata* (red circles) across East, South, and Southeast Asia

### Environmental variables

Environmental variables potentially influencing *Selaginella* distribution were compiled from publicly available global datasets and grouped into four categories: bioclimatic, edaphic, UVB radiation, and topographic factors (Table 1). All raster layers were resampled to 2.5 arc-minutes (~20.25 km² at the equator), clipped to the study area in ArcGIS 10.5, and converted to ASCII format for MaxEnt analysis. Historical (1970-2000) and future (2030, 2050, and 2080) climate data were obtained from WorldClim v2.1 (Fick and Hijmans 2017). An initial set of 26 candidate variables was screened for ecological relevance and subsequently filtered using Pearson correlation analysis to reduce multicollinearity. Variables with strong correlations ($|r| > 0.7$) were excluded (Dormann et al. 2013; Setyawan et al. 2018, 2021). Following screening, the final model retained 15 variables, including nine bioclimatic variables (bio_1, bio_4, bio_5, bio_6, bio_11, bio_12, bio_14, bio_16, and bio_17), two edaphic variables (soil organic carbon and soil pH) from ISRIC SoilGrids250m (Hengl et al. 2017), three UVB-related variables (uvb2, uvb3, and uvb4) from the gIUV database (Beckmann et al. 2014), and elevation derived from the SRTM digital elevation model (Farr et al. 2007). Together, these variables represented major thermal, hydrological, edaphic, radiation, and elevational gradients influencing habitat suitability and species distribution.

### Future climate scenarios

Future climate projections for 2030, 2050, and 2080 were obtained from the CIAT-CCAFS database, which provides downscaled and bias-corrected outputs from General Circulation Models (GCMs) (Navarro-Racines et al. 2020). The CCSM4 (Community Climate System Model version 4) model from the CMIP5 framework was selected because of its widespread use in species distribution modeling and its demonstrated applicability in tropical and subtropical regions. All climate layers were downloaded at a spatial resolution of 2.5 arc-minutes to match the environmental predictor datasets. Four Representative Concentration Pathways (RCPs) were evaluated: RCP 2.6, 4.5, 6.0, and 8.5 (IPCC 2021), representing a gradient from strong mitigation to high greenhouse-gas emissions. Future habitat suitability was projected for 2030, 2050, and 2080 to assess short- and long-term distributional responses of *S. kraussiana* and *S. uncinata* under contrasting climate-change scenarios. Because projections were based on a single GCM, uncertainty associated with differences among climate models was not explicitly evaluated.

### MaxEnt modeling

Species distribution models were developed using MaxEnt version 3.4.4 (Phillips et al. 2006; Phillips and Dudík 2008), a machine-learning algorithm widely used for presence-only species distribution modeling (Elith and Leathwick 2009; Elith et al. 2011). Separate models were generated for current climatic conditions (1970-2000) and future projections (2030, 2050, and 2080) under four RCP scenarios (2.6, 4.5, 6.0, and 8.5). Because true absence data were unavailable, 10,000 randomly generated background points were used to characterize environmental conditions across the study region (Phillips et al. 2006; Kramer-Schadt et al. 2016).

Default auto-feature settings were applied, and the regularization multiplier was set to 1 to reduce overfitting while maintaining ecological interpretability. Model calibration used a maximum of 5,000 iterations and a convergence threshold of $1 \times 10^{-5}$. Model performance and prediction variability were evaluated using 10-fold cross-validation, with 90% of occurrence records used for training and 10% for testing in each replicate. Clamping was disabled to minimize unrealistic extrapolation under novel future climates. Habitat suitability outputs were generated in complementary log-log (cloglog) format, which provides suitability values interpretable as relative probabilities of species occurrence (Khairunnisa et al. 2024).

**Table 1.** Environmental variables used in the MaxEnt model for predicting the distribution of *Selaginella kraussiana* and *S. uncinata* in East, South, and Southeast Asia

| Variable code | Environmental variable | Unit | Ecological relevance | Data source |
|---|---|---|---|---|
| bio_1 | Annual Mean Temperature | °C | Represents overall thermal conditions | WorldClim v2.1 |
| bio_4 | Temperature Seasonality | SD ×100 | Reflects annual temperature variability | WorldClim v2.1 |
| bio_5 | Maximum Temperature of Warmest Month | °C | Indicates upper thermal tolerance limits | WorldClim v2.1 |
| bio_6 | Minimum Temperature of Coldest Month | °C | Represents cold stress and frost limitation | WorldClim v2.1 |
| bio_11 | Mean Temperature of Coldest Quarter | °C | Reflects winter thermal suitability | WorldClim v2.1 |
| bio_12 | Annual Precipitation | mm | Represents long-term water availability | WorldClim v2.1 |
| bio_14 | Precipitation of Driest Month | mm | Indicates drought intensity | WorldClim v2.1 |
| bio_16 | Precipitation of Wettest Quarter | mm | Reflects moisture availability during peak rainfall | WorldClim v2.1 |
| bio_17 | Precipitation of Driest Quarter | mm | Represents seasonal drought stress | WorldClim v2.1 |
| soil_carbon | Soil Organic Carbon | g kg$^{-1}$ | Influences nutrient availability | ISRIC SoilGrids |
| soil_ph | Soil pH | pH | Affects nutrient solubility | ISRIC SoilGrids |
| uvb2 | UVB Seasonality | SD | Reflects temporal variation in UVB exposure | gIUV dataset |
| uvb3 | Mean UVB of Lightest Month | J m$^{-2}$ day$^{-1}$ | Represents peak UVB exposure conditions | gIUV dataset |
| uvb4 | Mean UVB of Lowest Month | J m$^{-2}$ day$^{-1}$ | Represents minimum seasonal UVB exposure | gIUV dataset |
| elev | Elevation | m asl | Represents topographic gradients | SRTM / WorldClim |

Note: Environmental variables were selected based on ecological relevance to *Selaginella* physiology and distribution, followed by Pearson correlation screening to reduce multicollinearity among predictor variables prior to MaxEnt modeling. Highly correlated variables ($|r| > 0.7$) were excluded during preliminary variable selection

### Model evaluation

Model performance was assessed using the Area Under the Receiver Operating Characteristic Curve (AUC), a threshold-independent measure of a model's ability to distinguish suitable from unsuitable conditions (Swets 1988; Allouche et al. 2006). Following Gorunescu (2011), AUC values <0.6 were considered poor, 0.6-0.7 weak, 0.7-0.8 fair, 0.8-0.9 good, and ≥0.9 excellent. Potential overfitting was evaluated by comparing training and test AUC values generated during cross-validation; differences >0.05 were considered indicative of overfitting (Warren and Seifert 2011). The relative importance of environmental variables was assessed using three complementary MaxEnt outputs: percent contribution, permutation importance, and jackknife analysis (Phillips et al. 2006). Percent contribution quantified the increase in model gain attributable to each predictor during training, permutation importance measured the decline in model performance after randomizing predictor values, and jackknife analysis evaluated the unique explanatory value of each variable by comparing models built with and without individual predictors.

### Spatial and statistical analysis

Habitat suitability maps were generated by importing MaxEnt output rasters into ArcGIS 10.5 for visualization and spatial analysis. Suitability values ranged from 0 (unsuitable) to 1 (highly suitable) and were reclassified into four categories following previous *Selaginella* studies (Setyawan et al. 2018, 2021): very low (0-0.2), low (0.2-0.4), medium (0.4-0.6), and high suitability (0.6-1.0). To improve area estimation accuracy, all raster layers were projected into the Asia North Albers Equal Area Conic coordinate system, and oceanic and non-terrestrial pixels were masked using a land polygon layer. Habitat area ($10^6$ km$^2$) was calculated separately for each suitability class and for total suitable habitat, defined as the combined area of low, medium, and high suitability classes, using the Zonal Geometry tool in ArcGIS. Changes in suitable habitat area were calculated as ΔArea = Area_future − Area_current, where positive values indicate expansion and negative values indicate contraction. All area estimates reported in Table 4 represent mean values derived from the 10-fold cross-validation replicates, and variability among replicates was generally low (typically <10% of the mean), indicating consistent model predictions across folds.

Pearson correlation analysis was conducted in R 4.2.0 using the "corrplot" package (Wei and Simko 2021; R Core Team 2022) to evaluate relationships among environmental variables and reduce multicollinearity prior to model calibration. Variables with strong correlations ($|r| > 0.7$) were screened, and retention was based on ecological relevance, contribution stability during preliminary model testing, and interpretability within the context of *Selaginella* ecology (Dormann et al. 2013). All statistical analyses were performed at $\alpha = 0.05$.

## RESULTS AND DISCUSSION

### Model accuracy-AUC

The performance of the MaxEnt models for both *Selaginella* species was evaluated using the Area Under the Receiver Operating Characteristic Curve (AUC) based on the current occurrence data. Both species exhibited excellent predictive performance for the current distribution models, with AUC values of 0.935 for *S. kraussiana* and 0.966 for *S. uncinata* (Figure 2; Table 2).

For *S. kraussiana*, the current distribution model achieved an AUC value of 0.935 (Figure 2.A), indicating excellent predictive performance. Differences between training and test AUC values remained small (≤0.028), suggesting limited overfitting and effective model calibration through spatial thinning and cross-validation procedures (Warren and Seifert 2011).

For *S. uncinata*, the current model yielded an AUC value of 0.966 (Figure 2.B), also indicating excellent predictive performance. Training-test AUC differences remained very low (≤0.012), indicating robust model calibration and strong predictive stability. The consistently high AUC values suggest that the selected environmental variables effectively captured the ecological requirements of both species.

Overall, the high AUC values obtained for both species indicate that the MaxEnt models provided reliable predictions of potential habitat suitability under current climatic conditions, and the same calibrated models were subsequently used to project future distributions under different climate scenarios.

## Variable contribution

The relative contribution of environmental variables differed substantially between *S. kraussiana* and *S. uncinata*, indicating contrasting ecological responses to climatic and environmental gradients across Asia (Table 3; Figure 3). Figure 3 presents the jackknife results for the current-climate (baseline) models, whereas Table 3 summarizes the percentage contributions of environmental variables for the current model and all future projections under RCP 2.6, 4.5, 6.0, and 8.5 in 2030, 2050, and 2080. Although the dominant predictors remained broadly associated with temperature and moisture availability, the relative importance of individual variables varied among climate scenarios, particularly under high-emission projections. Therefore, only the baseline jackknife results are presented to facilitate interpretation of the primary environmental drivers, while scenario-specific contributions are summarized in Table 3.

For *S. kraussiana*, temperature-related variables consistently represented the dominant predictors under both current and future climate scenarios. Under current climatic conditions, the most influential variables were the minimum temperature of the coldest month (bio_6), the precipitation of the driest month (bio_14), and the maximum temperature of the warmest month (bio_5). Annual mean temperature (bio_1) also contributed substantially, indicating that the species is strongly associated with thermal conditions and seasonal moisture availability. Under the moderate-emission scenario RCP 2.6 (2050), the overall contribution pattern remained broadly similar, with temperature and dry-season precipitation variables continuing to dominate the model.

Under future climate projections, particularly under the high-emission scenario RCP 8.5, the predicted distribution patterns suggested that cold-temperature limitations may become less restrictive for *S. kraussiana*, while seasonal radiation regimes and topographic gradients may play a greater role in shaping climatically suitable habitats. These projected patterns indicate that severe warming could facilitate the expansion of suitable habitat into regions that are currently constrained by low temperatures. Nevertheless, temperature- and moisture-related variables remained the primary environmental factors associated with the potential distribution of the species.

*Selaginella uncinata* exhibited an environmental response pattern dominated primarily by moisture-related variables. Annual precipitation (bio_12) consistently represented the strongest predictor across all scenarios, while UVB seasonality (uvb2), temperature seasonality (bio_4), and mean temperature of the coldest quarter (bio_11) also contributed substantially to model performance. Precipitation of the driest month (bio_14) showed moderate influence, whereas edaphic variables such as soil organic carbon and soil pH contributed minimally across all climate scenarios. Unlike *S. kraussiana*, the relative importance of major predictors remained remarkably stable across all RCPs and time periods, indicating greater ecological consistency in the species' response to future climatic conditions. These results indicate that *S. uncinata* is more strongly associated with hydrological stability and persistently humid environments than with temperature extremes alone.

The jackknife analysis further supported these contrasting ecological patterns (Figure 3). For *S. kraussiana*, the minimum temperature of the coldest month (bio_6) and precipitation of the driest month (bio_14) contained the highest unique explanatory information, indicating stronger dependence on winter temperature and seasonal moisture conditions. *Selaginella uncinata* was more strongly associated with annual precipitation (bio_12) and temperature seasonality (bio_4), emphasizing the importance of stable humid habitats for its persistence. The results indicate that *S. kraussiana* appears more strongly constrained by thermal variables, whereas *S. uncinata* shows greater association with precipitation-related environmental stability, differences that likely influence their contrasting responses to future climate change.

## Current distribution

For *S. kraussiana* (Figure 4.A), suitable habitat is concentrated in tropical and subtropical regions of Asia, including southern China, northeastern India, mainland Southeast Asia (Myanmar, Thailand, Vietnam, Laos, and Cambodia), the Malay Peninsula, and the Indonesian archipelago (Sumatra, Java, and Borneo). High-suitability areas occur primarily in humid tropical and subtropical regions, particularly southern China, mainland Southeast Asia, and montane areas of the Indonesian archipelago. In contrast, large portions of East Asia, including northern China, the Korean Peninsula, and Japan, are classified as having very low suitability, likely reflecting the strong influence of the minimum temperature of the coldest month (bio_6), the most important predictor in the current model. The current distribution encompasses approximately 11.47 × $10^6$ $km^2$ of suitable habitat (combined low-, medium-, and high-suitability classes) across the study region (Table 4.A).

For *S. uncinata* (Figure 4.B), the current distribution is more restricted than that of *S. kraussiana*. High-suitability areas are concentrated in southern China (Yunnan, Guangxi, and Guangdong), Taiwan, and the Himalayan foothills (Nepal, Bhutan, and northeastern India). Unlike *S. kraussiana*, *S. uncinata* exhibits limited suitability across much of lowland Southeast Asia and the Indonesian archipelago, with suitable habitat primarily associated with humid montane and subtropical environments. The predicted distribution corresponds closely with the strong influence of annual precipitation (bio_12) and temperature seasonality (bio_4), indicating a greater dependence on stable moisture conditions. Several montane areas in West Java were also identified as suitable habitat, consistent with previous reports of naturalized populations in the region (Setyawan 2014). The total suitable habitat area for *S. uncinata* was estimated at approximately 2.95 × $10^6$ km² (Table 4.B), substantially smaller than the 11.47 × $10^6$ km² estimated for *S. kraussiana* under current climatic conditions.

**Table 2.** Model performance evaluation (AUC values) for *Selaginella kraussiana* and *S. uncinata*

| Species | Scenario | AUC value | Classification | Training AUC | Test AUC | Difference |
|---|---|---|---|---|---|---|
| *S. kraussiana* | Current | 0.935 | Excellent | 0.942 | 0.928 | 0.014 |
| *S. uncinata* | Current | 0.966 | Excellent | 0.972 | 0.960 | 0.012 |

Note: Classification criteria: AUC < 0.6 = Fail, 0.6-0.7 = Poor, 0.7-0.8 = Fair, 0.8-0.9 = Good, AUC ≥ 0.9 = Excellent (Gorunescu 2011)

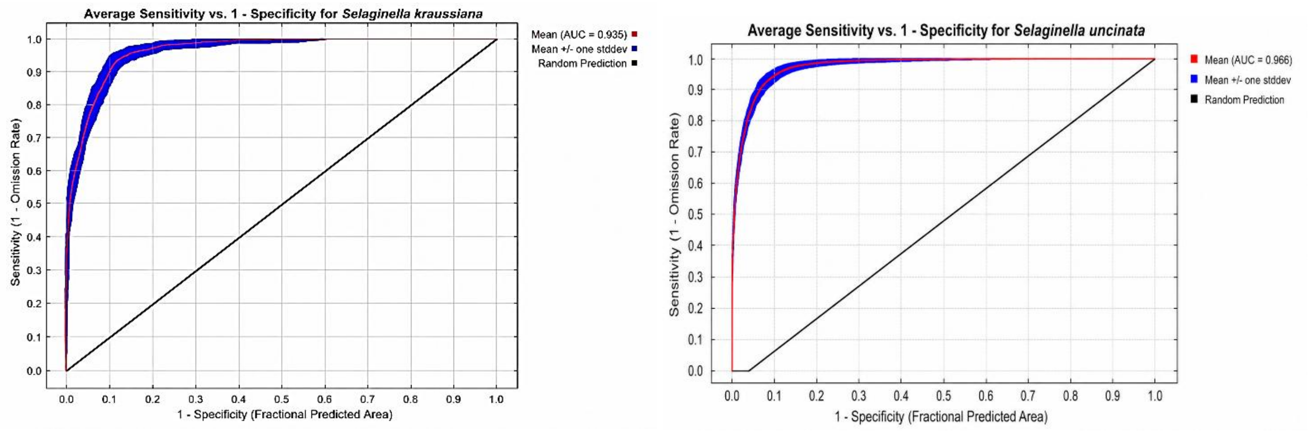

A

B

**Figure 2.** ROC curves of the current MaxEnt models for *Selaginella kraussiana* (A) and *S. uncinata* (B)

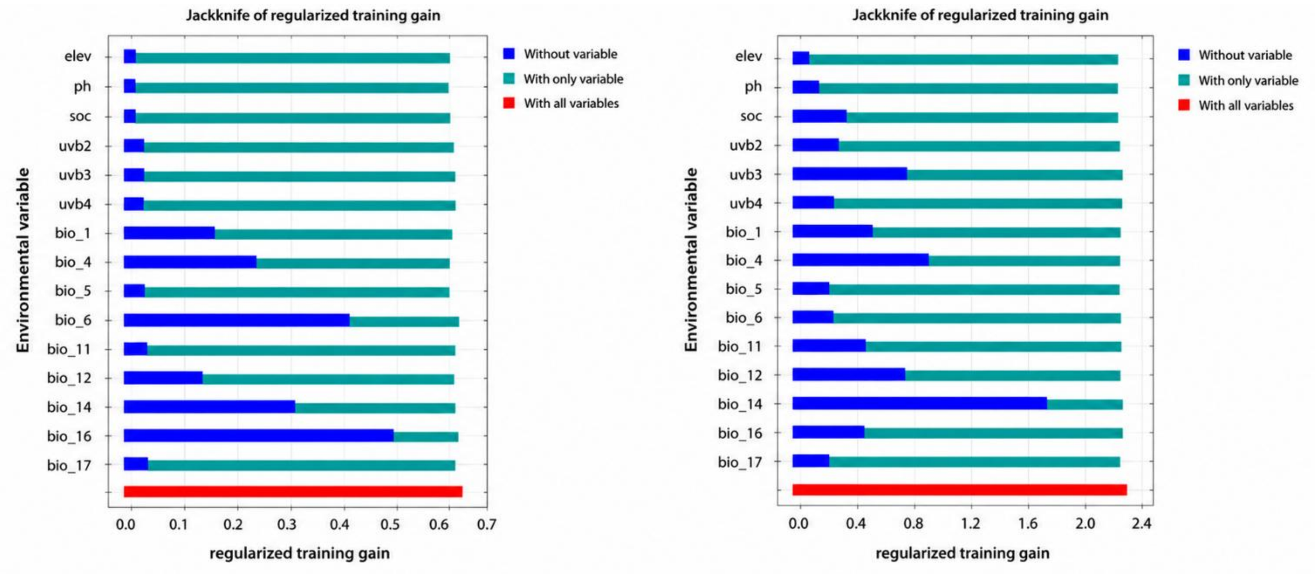

A

B

**Figure 3.** Jackknife test of environmental variable importance for the current-climate MaxEnt models of *Selaginella kraussiana* (A) and *S. uncinata* (B). Bars indicate model gain when each variable is used in isolation (blue) and when omitted from the full model (cyan). Red bars represent the gain of the complete model

**Table 3.** Relative contribution (%) of environmental variables to the MaxEnt models for *Selaginella kraussiana* and *S. uncinata* under current and future climate scenarios

| Variable code | Environmental variable | Current | RCP 2.6 (2030) | RCP 4.5 (2030) | RCP 6.0 (2030) | RCP 8.5 (2030) | RCP 2.6 (2050) | RCP 4.5 (2050) | RCP 6.0 (2050) | RCP 8.5 (2050) | RCP 2.6 (2080) | RCP 4.5 (2080) | RCP 6.0 (2080) | RCP 8.5 (2080) |
|---|---|---|---|---|---|---|---|---|---|---|---|---|---|---|
| **A. *S. kraussiana*** | | | | | | | | | | | | | | |
| bio_1 | Annual Mean Temperature | 13.0 | 13.1 | 12.9 | 12.4 | 11.2 | 13.2 | 11.6 | 10.9 | 10.1 | 12.7 | 11.2 | 10.3 | 9.4 |
| bio_4 | Temperature Seasonality | 6.3 | 6.5 | 5.9 | 6.1 | 5.6 | 6.7 | 5.8 | 5.5 | 5.2 | 6.3 | 5.6 | 5.3 | 4.8 |
| bio_5 | Maximum Temperature of Warmest Month | 14.4 | 13.6 | 12.8 | 12.3 | 11.7 | 13.1 | 12.1 | 11.4 | 10.3 | 12.6 | 11.5 | 10.6 | 9.7 |
| bio_6 | Minimum Temperature of Coldest Month | 31.6 | 30.5 | 28.7 | 26.9 | 24.2 | 29.8 | 26.2 | 23.5 | 20.6 | 28.6 | 24.1 | 21.0 | 17.4 |
| bio_11 | Mean Temperature of Coldest Quarter | 3.7 | 3.9 | 4.1 | 4.3 | 4.6 | 4.0 | 4.4 | 4.7 | 5.0 | 4.2 | 4.7 | 5.0 | 5.4 |
| bio_12 | Annual Precipitation | 2.1 | 2.3 | 2.5 | 2.7 | 3.1 | 2.6 | 2.9 | 3.2 | 3.7 | 2.7 | 3.2 | 3.6 | 4.1 |
| bio_14 | Precipitation of Driest Month | 24.3 | 22.7 | 21.0 | 19.3 | 17.2 | 21.9 | 19.3 | 16.6 | 13.5 | 21.0 | 17.3 | 14.2 | 11.2 |
| bio_16 | Precipitation of Wettest Quarter | 1.8 | 2.0 | 2.1 | 2.4 | 2.6 | 2.2 | 2.5 | 2.8 | 3.1 | 2.3 | 2.7 | 3.0 | 3.4 |
| bio_17 | Precipitation of Driest Quarter | 1.5 | 1.6 | 1.8 | 2.0 | 2.3 | 1.8 | 2.1 | 2.4 | 2.8 | 1.9 | 2.3 | 2.6 | 3.0 |
| soil_carbon | Soil Organic Carbon | 1.2 | 1.4 | 1.3 | 1.6 | 1.8 | 1.4 | 1.7 | 1.9 | 2.2 | 1.5 | 1.8 | 2.1 | 2.4 |
| soil_ph | Soil pH | 0.9 | 0.9 | 1.0 | 1.2 | 1.3 | 1.1 | 1.2 | 1.4 | 1.7 | 1.1 | 1.4 | 1.6 | 1.9 |
| uvb2 | UVB Seasonality | 1.8 | 2.1 | 2.6 | 3.2 | 3.9 | 2.4 | 3.2 | 4.2 | 5.4 | 2.7 | 4.0 | 5.2 | 6.8 |
| uvb3 | Mean UVB of Lightest Month | 0.7 | 0.8 | 1.0 | 1.1 | 1.3 | 0.9 | 1.1 | 1.3 | 1.7 | 1.0 | 1.3 | 1.5 | 1.9 |
| uvb4 | Mean UVB of Lowest Month | 0.5 | 0.6 | 0.9 | 1.0 | 1.2 | 0.7 | 1.1 | 1.4 | 1.8 | 0.8 | 1.4 | 1.7 | 2.3 |
| elev | Elevation | 0.3 | 0.4 | 0.7 | 1.0 | 1.3 | 0.5 | 1.0 | 1.4 | 2.0 | 0.7 | 1.3 | 1.9 | 2.7 |
| | | 100.0 | 100.1 | 99.9 | 100.0 | 100.1 | 99.9 | 100.1 | 100.0 | 99.9 | 100.1 | 100.0 | 100.1 | 100.0 |
| **B. *S. uncinata*** | | | | | | | | | | | | | | |
| bio_1 | Annual Mean Temperature | 5.1 | 5.0 | 4.7 | 4.9 | 4.4 | 4.9 | 4.5 | 4.3 | 4.0 | 4.8 | 4.3 | 4.1 | 3.8 |
| bio_4 | Temperature Seasonality | 14.6 | 14.2 | 13.9 | 13.6 | 13.3 | 14.0 | 13.4 | 13.0 | 12.5 | 13.7 | 13.0 | 12.6 | 12.1 |
| bio_5 | Maximum Temperature of Warmest Month | 2.4 | 2.2 | 2.1 | 2.2 | 2.0 | 2.1 | 2.0 | 1.9 | 1.8 | 2.1 | 1.9 | 1.8 | 1.6 |
| bio_6 | Minimum Temperature of Coldest Month | 6.5 | 6.2 | 5.9 | 5.8 | 5.5 | 5.9 | 5.6 | 5.4 | 5.1 | 5.7 | 5.4 | 5.1 | 4.8 |
| bio_11 | Mean Temperature of Coldest Quarter | 13.0 | 12.6 | 12.4 | 12.2 | 11.9 | 12.4 | 12.0 | 11.7 | 11.3 | 12.1 | 11.7 | 11.4 | 10.9 |
| bio_12 | Annual Precipitation | 39.5 | 40.0 | 40.5 | 40.9 | 41.5 | 40.4 | 41.1 | 41.8 | 42.7 | 40.9 | 41.7 | 42.5 | 43.5 |
| bio_14 | Precipitation of Driest Month | 8.7 | 8.3 | 8.0 | 7.6 | 7.2 | 8.0 | 7.5 | 7.0 | 6.5 | 7.7 | 7.1 | 6.6 | 6.0 |
| bio_16 | Precipitation of Wettest Quarter | 3.2 | 3.2 | 3.3 | 3.4 | 3.5 | 3.4 | 3.5 | 3.7 | 3.8 | 3.4 | 3.7 | 3.8 | 4.0 |
| bio_17 | Precipitation of Driest Quarter | 2.9 | 2.9 | 3.0 | 3.2 | 3.3 | 3.1 | 3.3 | 3.4 | 3.6 | 3.2 | 3.4 | 3.6 | 3.8 |
| soil_carbon | Soil Organic Carbon | 0.8 | 0.7 | 0.7 | 0.8 | 0.6 | 0.7 | 0.6 | 0.6 | 0.5 | 0.6 | 0.6 | 0.5 | 0.5 |
| soil_ph | Soil pH | 0.5 | 0.4 | 0.4 | 0.4 | 0.4 | 0.4 | 0.4 | 0.3 | 0.3 | 0.4 | 0.3 | 0.3 | 0.3 |
| uvb2 | UVB Seasonality | 18.6 | 19.2 | 19.8 | 20.5 | 21.3 | 19.6 | 20.5 | 21.3 | 22.4 | 20.0 | 21.5 | 22.3 | 23.2 |
| uvb3 | Mean UVB of Lightest Month | 1.2 | 1.1 | 1.0 | 0.9 | 0.8 | 1.0 | 0.8 | 0.8 | 0.7 | 0.9 | 0.8 | 0.7 | 0.7 |
| uvb4 | Mean UVB of Lowest Month | 0.9 | 0.9 | 1.0 | 1.1 | 1.2 | 1.0 | 1.1 | 1.2 | 1.4 | 1.1 | 1.2 | 1.4 | 1.5 |
| elev | Elevation | 1.4 | 1.5 | 1.6 | 1.8 | 1.9 | 1.6 | 1.8 | 2.1 | 2.3 | 1.7 | 2.1 | 2.3 | 2.5 |
| | | 100.0 | 100.1 | 100.1 | 100.0 | 100.1 | 100.0 | 100.0 | 100.1 | 99.9 | 100.0 | 99.9 | 100.1 | 100.0 |

Note: Only variables retained after Pearson correlation filtering were included in the final MaxEnt models. Percent contribution values indicate the relative influence of each environmental predictor during model training. Variable contributions are consistent with the environmental dataset summarized in Table 1, the jackknife results in Figure 3, and the ecological interpretations presented in the text. Totals may differ slightly due to rounding

**Table 4.** Changes in suitable habitat area (×$10^6$ km²) for *Selaginella kraussiana* and *S. uncinata* under current and future climate scenarios

| **Suitability class** | **Current** | **RCP2.6 2030** | **Change** | **RCP4.5 2030** | **Change** | **RCP6.0 2030** | **Change** | **RCP8.5 2030** | **Change** | **RCP2.6 2050** | **Change** | **RCP4.5 2050** | **Change** | **RCP6.0 2050** | **Change** | **RCP8.5 2050** | **Change** | **RCP2.6 2080** | **Change** | **RCP4.5 2080** | **Change** | **RCP6.0 2080** | **Change** | **RCP8.5 2080** | **Change** |
|---|---|---|---|---|---|---|---|---|---|---|---|---|---|---|---|---|---|---|---|---|---|---|---|---|---|
| **A. *S. kraussiana*** | | | | | | | | | | | | | | | | | | | | | | | | | |
| Very Low | 10.03 | 9.78 | -0.25 | 9.38 | -0.65 | 8.90 | -1.13 | 7.95 | -2.08 | 9.68 | -0.35 | 8.63 | -1.40 | 7.69 | -2.34 | 6.13 | -3.90 | 9.55 | -0.48 | 7.90 | -2.13 | 6.40 | -3.63 | 4.98 | -5.05 |
| Low | 5.85 | 5.92 | +0.07 | 6.13 | +0.28 | 6.41 | +0.56 | 6.99 | +1.14 | 5.95 | +0.10 | 6.52 | +0.67 | 7.36 | +1.51 | 8.60 | +2.75 | 6.02 | +0.17 | 7.04 | +1.19 | 8.06 | +2.21 | 9.15 | +3.30 |
| Medium | 2.76 | 2.88 | +0.12 | 3.02 | +0.26 | 3.17 | +0.41 | 3.38 | +0.62 | 2.90 | +0.14 | 3.21 | +0.45 | 3.60 | +0.84 | 3.98 | +1.22 | 2.93 | +0.17 | 3.35 | +0.59 | 3.73 | +0.97 | 3.99 | +1.23 |
| High | 2.86 | 2.92 | +0.06 | 2.97 | +0.11 | 3.05 | +0.19 | 3.18 | +0.32 | 2.97 | +0.11 | 3.15 | +0.29 | 3.28 | +0.42 | 3.32 | +0.46 | 3.00 | +0.14 | 3.16 | +0.30 | 3.27 | +0.41 | 3.29 | +0.43 |
| Total Suitable | 11.47 | 11.72 | +0.25 | 12.12 | +0.65 | 12.63 | +1.16 | 13.55 | +2.08 | 11.82 | +0.35 | 12.88 | +1.41 | 14.24 | +2.77 | 15.90 | +4.43 | 11.95 | +0.48 | 13.55 | +2.08 | 15.06 | +3.59 | 16.43 | +4.96 |
| **B. *S. uncinata*** | | | | | | | | | | | | | | | | | | | | | | | | | |
| Very Low | 18.55 | 18.47 | -0.08 | 18.43 | -0.12 | 18.36 | -0.19 | 18.18 | -0.37 | 18.45 | -0.10 | 18.29 | -0.26 | 18.14 | -0.41 | 17.87 | -0.68 | 18.42 | -0.13 | 18.24 | -0.31 | 18.05 | -0.50 | 17.66 | -0.89 |
| Low | 0.95 | 0.92 | -0.03 | 0.93 | -0.02 | 0.94 | -0.01 | 0.97 | +0.02 | 0.89 | -0.06 | 0.95 | 0.00 | 0.97 | +0.02 | 1.00 | +0.05 | 0.91 | -0.04 | 0.96 | +0.01 | 0.99 | +0.04 | 1.02 | +0.07 |
| Medium | 0.68 | 0.70 | +0.02 | 0.71 | +0.03 | 0.72 | +0.04 | 0.74 | +0.06 | 0.72 | +0.04 | 0.75 | +0.07 | 0.77 | +0.09 | 0.80 | +0.12 | 0.73 | +0.05 | 0.76 | +0.08 | 0.79 | +0.11 | 0.81 | +0.13 |
| High | 1.32 | 1.31 | -0.01 | 1.29 | -0.03 | 1.28 | -0.04 | 1.27 | -0.05 | 1.29 | -0.03 | 1.27 | -0.05 | 1.25 | -0.07 | 1.22 | -0.10 | 1.28 | -0.04 | 1.26 | -0.06 | 1.24 | -0.08 | 1.21 | -0.11 |
| Total Suitable | 2.95 | 2.93 | -0.02 | 2.93 | -0.02 | 2.94 | -0.01 | 2.98 | +0.03 | 2.90 | -0.05 | 2.97 | +0.02 | 2.99 | +0.04 | 3.02 | +0.07 | 2.92 | -0.03 | 2.98 | +0.03 | 3.02 | +0.07 | 3.04 | +0.09 |

Note: Area values are expressed in ×$10^6$ km² and were calculated using terrestrial pixels only after masking oceanic regions within an equal-area projection framework. Total Suitable represents the combined area of the low (0.2-0.4), medium (0.4-0.6), and high (0.6-1.0) suitability classes. Areas with suitability values <0.2 were classified as Very Low suitability and considered unsuitable habitat. Change was calculated as Future-Current; positive values indicate habitat expansion, whereas negative values indicate habitat contraction or a reduction in unsuitable habitat area. Minor discrepancies in totals may occur due to rounding

### Future distribution projections

Future distribution shifts for both species were projected for 2030, 2050, and 2080 under four RCP scenarios (2.6, 4.5, 6.0, and 8.5). Figures 5 and 6 illustrate the projected redistribution patterns, revealing contrasting responses of the two species to future climate change.

For *S. kraussiana* (Figure 5), future projections indicate a progressive expansion of climatically suitable habitat under all climate scenarios. Total suitable habitat increased from 11.47 × $10^6$ km$^2$ under current conditions to between 11.72 and 16.43 × $10^6$ km$^2$ across future scenarios, with the magnitude of expansion generally increasing with emission intensity and projection period (Table 4). Under RCP 2.6, habitat expansion was relatively modest and characterized by gradual increases in suitability across southern China, mainland Southeast Asia, and parts of the Indonesian archipelago. Under the intermediate scenarios (RCP 4.5 and 6.0), expansion became more pronounced, particularly in subtropical and montane regions, while some lowland tropical areas exhibited reduced suitability. These patterns suggest a gradual expansion of climatically suitable habitat into higher-latitude and higher-elevation regions.

Under the high-emission scenario RCP 8.5, projected changes became substantially more pronounced. By 2080, total suitable habitat reached 16.43 × $10^6$ km$^2$, representing an increase of 4.96 × $10^6$ km$^2$ relative to current conditions (Table 4). Although climatic suitability declined in some tropical lowland regions, extensive areas of East Asia and many higher-elevation regions were projected to become increasingly suitable. The expansion of suitable habitat into subtropical and temperate environments is consistent with the declining influence of cold-temperature constraints observed in the variable contribution analysis and suggests that future warming may facilitate a substantial broadening of the potential climatic niche of *S. kraussiana*.

In contrast, *S. uncinata* (Figure 6) exhibited comparatively stable distribution patterns across all future climate scenarios. Suitable habitat remained concentrated within its current core distribution regions, particularly southern China, Taiwan, and the Himalayan foothills. Total suitable habitat increased only slightly from 2.95 × $10^6$ km$^2$ under current conditions to 3.04 × $10^6$ km$^2$ under RCP 8.5 in 2080 (Table 4), indicating relatively limited sensitivity to projected climate change compared with *S. kraussiana*.

Under RCP 2.6, minor expansions were projected in several montane regions of East and Southeast Asia, whereas under RCP 8.5, small contractions occurred near some distribution margins and were offset by localized gains in climatically suitable habitat elsewhere. Overall, the geographic distribution of *S. uncinata* remained remarkably stable across all RCPs and time periods. This pattern is consistent with the species' strong association with annual precipitation and humid environmental conditions, suggesting that suitable habitats are likely to persist despite projected climatic changes. Unlike *S. kraussiana*, *S. uncinata* showed little evidence of pronounced expansion into higher-latitude regions, indicating greater climatic stability within persistently humid regions.

### Pearson correlation analysis

Pearson correlation analysis was performed as a preliminary variable-screening procedure prior to final MaxEnt model calibration (Figure 7). The analysis included the complete set of candidate environmental predictors representing bioclimatic, edaphic, UVB-radiation, and topographic factors. Variables exhibiting strong pairwise correlations ($|r| > 0.7$) were considered potentially collinear following Dormann et al. (2013).

Several highly correlated predictor pairs were identified, particularly among temperature- and UVB-related variables. For example, bio_5 and bio_9 ($r = -0.98$) in *S. kraussiana*, bio_6 and bio_9 ($r = 0.93$) in *S. uncinata*, and uvb1 and uvb2 ($r > 0.80$ in both species) showed strong correlations. To reduce multicollinearity and improve model interpretability, bio_9 and uvb1 were excluded from the final set of predictors. Following this screening process, 15 environmental variables were retained for the final MaxEnt models, including 9 bioclimatic variables (bio_1, bio_4, bio_5, bio_6, bio_11, bio_12, bio_14, bio_16, and bio_17), 2 edaphic variables (soil organic carbon and soil pH), 3 UVB-radiation variables (uvb2, uvb3, and uvb4), and 1 topographic variable (elevation). These retained variables were subsequently used for all current and future projections under RCP 2.6, 4.5, 6.0, and 8.5 for 2030, 2050, and 2080.

### Area change analysis

Quantitative changes in suitable habitat area for both species under current and future climate scenarios are summarized in Table 4, with Table 4.A represents *S. kraussiana* and Table 4.B represents *S. uncinata*. Habitat area values are expressed in $10^6$ km$^2$ across four suitability classes. Area calculations were based exclusively on terrestrial pixels after masking marine regions and non-land surfaces, and all analyses were conducted using an equal-area projection system to minimize spatial distortion across the study region. Variability among cross-validation replicates was generally low (typically <10% of the mean), indicating consistent model predictions across folds.

For *S. kraussiana*, the current suitable habitat (combined low-, medium-, and high-suitability classes) was estimated at 11.47 × $10^6$ km$^2$. Future projections indicated consistent habitat expansion across all RCP scenarios and projection periods (Table 4.A). Under RCP 2.6, total suitable habitat increased modestly to 11.72 × $10^6$ km$^2$ in 2030, 11.82 × $10^6$ km$^2$ in 2050, and 11.95 × $10^6$ km$^2$ in 2080. In contrast, substantially greater expansion was projected under intermediate- and high-emission scenarios. Under RCP 8.5, total suitable habitat increased to 13.55 × $10^6$ km$^2$ in 2030, 15.90 × $10^6$ km$^2$ in 2050, and 16.43 × $10^6$ km$^2$ in 2080, representing a net gain of 4.96 × $10^6$ km$^2$ relative to current conditions. Habitat expansion was particularly evident within the low- and medium-suitability classes, whereas the area classified as very low suitability declined progressively across future scenarios. These results indicate substantial geographic expansion and redistribution of climatically suitable habitat under future warming conditions.

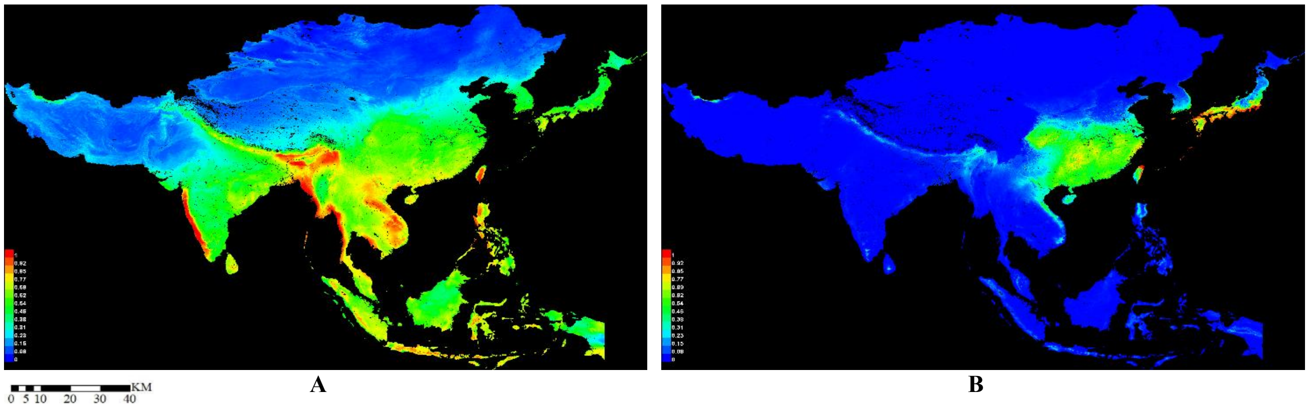

**Figure 4.** Current suitable habitat distribution of *Selaginella kraussiana* (A) and *S. uncinata* (B). Habitat suitability is classified into four categories: very low (0-0.2; blue), low (0.2-0.4; light blue/green), medium (0.4-0.6; green), and high (0.6-1.0; yellow/red)

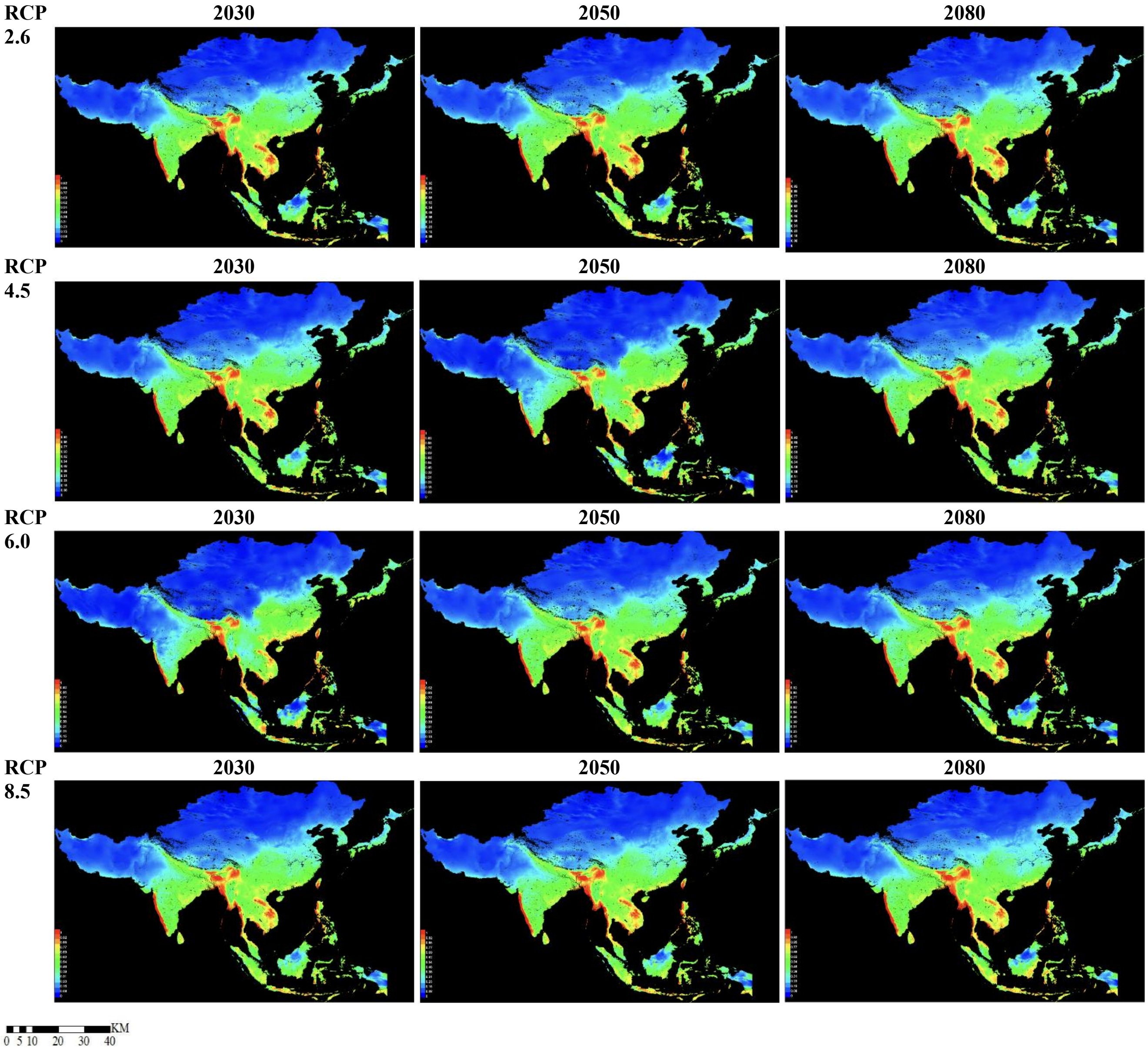

**Figure 5.** Future distribution shifts of *Selaginella kraussiana* under RCP 2.6, 4.5, 6.0, and 8.5 (2030, 2050, 2080). Habitat suitability is classified into four categories: very low (0-0.2; blue), low (0.2-0.4; light blue/green), medium (0.4-0.6; green), and high (0.6-1.0; yellow/red)

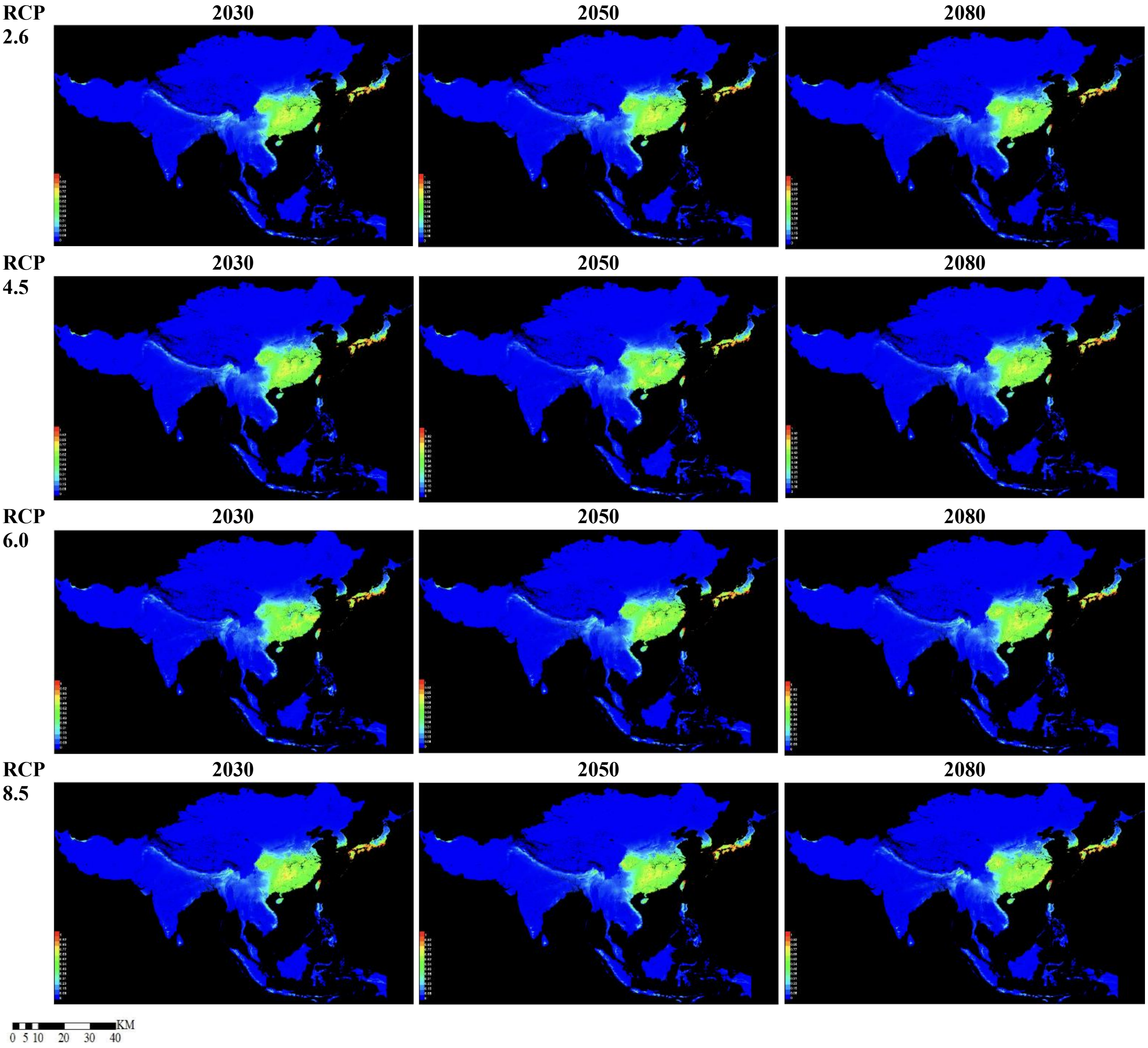

**Figure 6.** Future distribution shifts of *Selaginella uncinata* under RCP 2.6, 4.5, 6.0, and 8.5 (2030, 2050, 2080). Habitat suitability is classified into four categories: very low (0-0.2; blue), low (0.2-0.4; light blue/green), medium (0.4-0.6; green), and high (0.6-1.0; yellow/red)

For *S. uncinata*, changes in suitable habitat area were comparatively limited across all future climate scenarios. Current suitable habitat was estimated at approximately 2.95 × $10^6$ km$^2$, substantially smaller than that of *S. kraussiana*. Across all RCP scenarios, total suitable habitat remained remarkably stable, ranging from 2.90 to 3.04 × $10^6$ km$^2$. Under RCP 8.5, total suitable habitat increased only slightly from 2.95 × $10^6$ km$^2$ under current conditions to 2.98 × $10^6$ km$^2$ in 2030, 3.02 × $10^6$ km$^2$ in 2050, and 3.04 × $10^6$ km$^2$ in 2080 (Table 4.B). Small increases in low- and medium-suitability areas were accompanied by slight reductions in highly suitable habitat, resulting in only minor net changes in overall habitat extent. The relatively small magnitude of change suggests that the climatic niche of *S. uncinata* is likely to remain largely stable under projected future climates.

The magnitude of projected distributional change was therefore substantially greater for *S. kraussiana* than for *S. uncinata*, indicating contrasting responses to future climate change. Whereas *S. kraussiana* exhibited progressive habitat expansion that intensified with increasing emission levels and longer projection periods, *S. uncinata* showed only marginal changes in suitable habitat area across all RCP scenarios and time horizons. Figure 8 illustrates these contrasting patterns, showing pronounced habitat expansion for *S. kraussiana*, particularly under RCP 8.5, whereas *S. uncinata* exhibited comparatively limited spatial redistribution throughout the projection period.

## Discussion

### *Key environmental drivers*

The MaxEnt models revealed distinct environmental controls on the distributions of *S. kraussiana* and *S. uncinata*, indicating contrasting ecological niches and responses to climate change (Table 3; Figure 3). For *S. kraussiana*, temperature-related variables dominated the current model, particularly the minimum temperature of the coldest month (bio_6), followed by precipitation of the driest month (bio_14), maximum temperature of the warmest month (bio_5), and annual mean temperature (bio_1). These results suggest that winter temperature and seasonal moisture availability are the primary factors limiting the species' distribution. Such associations are consistent with its occurrence in humid tropical and warm-temperate regions and its sensitivity to frost and prolonged drought (Gola and Jernstedt 2016; Brownsey and Perrie 2018).

Future projections indicated changes in the relative importance of environmental predictors for *S. kraussiana*. Under increasingly severe climate scenarios, the contribution of cold-temperature variables, particularly the minimum temperature of the coldest month (bio_6), gradually declined, although they remained among the most influential predictors. In contrast, several variables related to UVB radiation and elevation showed moderate increases in relative contribution. Under RCP 8.5 in 2080, UVB seasonality (uvb2), UVB intensity variables, and elevation contributed more strongly than under current conditions, suggesting that radiation regimes, topographic gradients, and seasonal thermal stress may become increasingly relevant in shaping future habitat suitability. Nevertheless, temperature- and moisture-related variables continued to represent the primary environmental constraints governing the potential distribution of *S. kraussiana*.

In contrast, *S. uncinata* was consistently associated with moisture-related variables. Annual precipitation (bio_12) remained the dominant predictor across all climate scenarios, contributing 39.5-43.5% of the total predictor contribution, whereas UVB seasonality (uvb2), temperature seasonality (bio_4), and mean temperature of the coldest quarter (bio_11) served as important secondary predictors. This pattern is consistent with the species' preference for humid forest floors, shaded stream banks, and moist montane habitats (Li et al. 2022; Qin et al. 2022). Unlike *S. kraussiana*, the relative importance of environmental predictors remained remarkably stable across future scenarios, reflecting only minor changes in projected habitat suitability and geographic distribution.

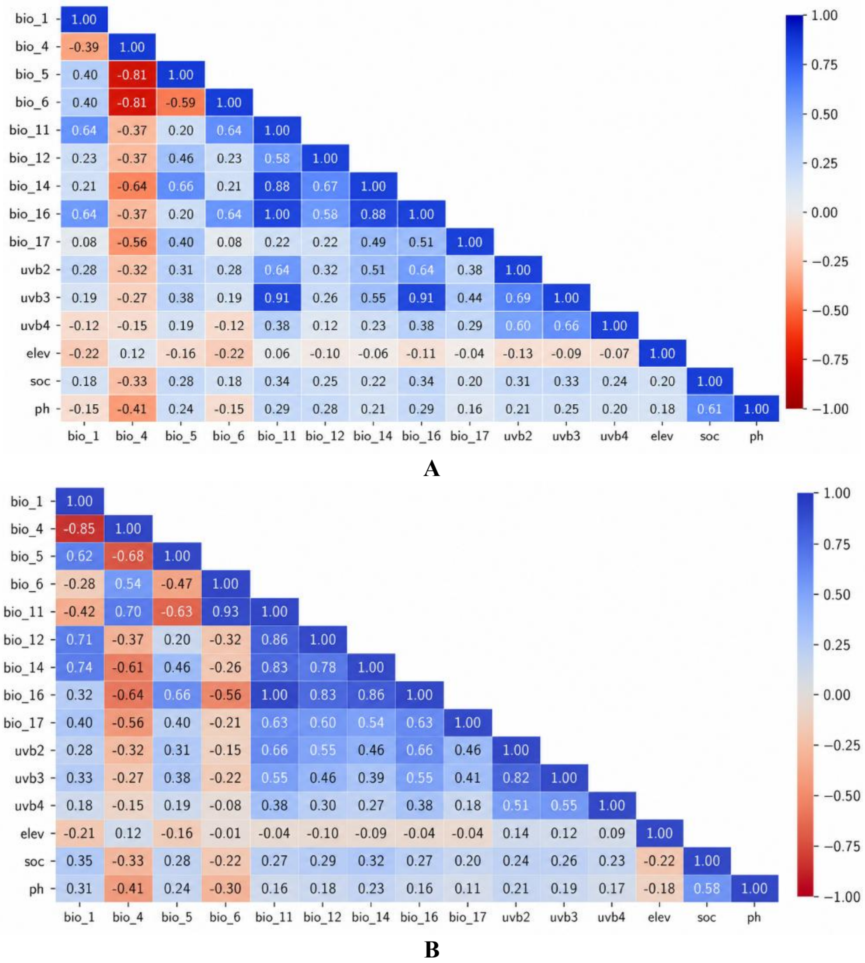

**Figure 7.** Pearson correlation matrices for environmental variables. A. *Selaginella kraussiana*, B. *Selaginella uncinata*

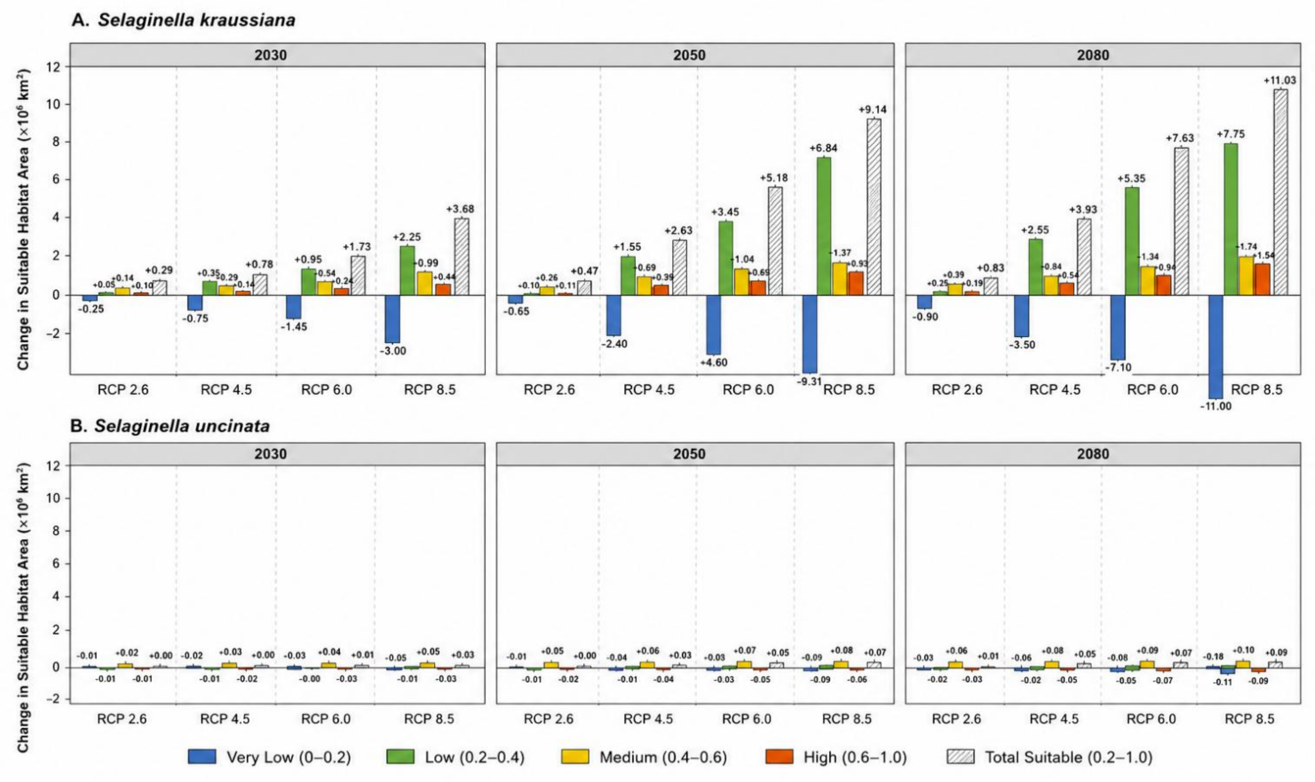

**Figure 8.** Projected changes in suitable habitat area (×10⁶ km²) across suitability classes for *Selaginella kraussiana* and *S. uncinata* under RCP 2.6, 4.5, 6.0, and 8.5 scenarios for 2030, 2050, and 2080. Positive values indicate increases in habitat area, whereas negative values indicate decreases relative to current conditions. Total Suitable represents the combined area of low (0.2-0.4), medium (0.4-0.6), and high (0.6-1.0) suitability classes

The jackknife analysis further supported these patterns. *Selaginella kraussiana* was most strongly associated with bio_6 and bio_14, whereas *S. uncinata* was primarily influenced by bio_12 and temperature seasonality (bio_4). Overall, *S. kraussiana* appears primarily constrained by thermal conditions but may become increasingly influenced by radiation and topographic factors under future climates, whereas *S. uncinata* remains strongly associated with precipitation-driven environmental stability.

### *Climate response of both species*

Future climate projections revealed contrasting responses between the two *Selaginella* species, indicating that closely related invasive taxa may differ substantially in their responses to climate change (Figures 5-6; Table 4). *Selaginella kraussiana* exhibited pronounced habitat expansion under future warming scenarios, whereas *S. uncinata* showed comparatively stable distribution patterns.

For *S. kraussiana*, total suitable habitat increased from $11.47 \times 10^6$ km² under current conditions to $16.43 \times 10^6$ km² under RCP 8.5 in 2080, representing an expansion of approximately 43% (Table 4). Habitat gains were concentrated in regions currently constrained by low winter temperatures, including northern China, the Korean Peninsula, and southern Japan. This pattern is consistent with the dominant influence of the minimum temperature of the coldest month (*bio_6*), suggesting that climate warming may reduce thermal barriers and facilitate range expansion into higher-latitude and higher-elevation regions (IPCC 2021). At the same time, some tropical lowland regions showed reduced suitability, indicating that excessive warming may limit habitat quality in parts of the current range. Future scenarios showed moderate increases in the relative contribution of UVB-related variables and elevation, suggesting a growing influence of radiation regimes and topographic factors on habitat suitability.

In contrast, *S. uncinata* exhibited relatively minor distributional changes across all climate scenarios. Highly suitable habitats in southern China, Taiwan, and other humid subtropical regions remained largely persistent. Total suitable habitat increased only marginally from $2.95 \times 10^6$ km² under current conditions to $3.04 \times 10^6$ km² under RCP 8.5 in 2080, representing a net gain of just $0.09 \times 10^6$ km² (Table 4). This limited change is consistent with the dominant influence of annual precipitation (*bio_12*) and the remarkable stability of environmental predictor contributions across future scenarios. The species appears more strongly constrained by hydrological conditions than by temperature, making it comparatively less sensitive to climate-driven range shifts.

Overall, climate warming is projected to substantially increase the potential distribution of *S. kraussiana*, whereas *S. uncinata* is expected to maintain a relatively stable distribution associated with persistently humid environments. These contrasting responses highlight the importance of species-specific risk assessment and management strategies for invasive plants under future climate change.

*Invasiveness implications in Asia*

These projected distributional shifts have important implications for the management of invasive *Selaginella* species in Asia, where both taxa are already cultivated or naturalized in several regions (Setyawan 2011, 2014; Dang et al. 2019). Climate change may increase invasion risk by expanding climatically suitable habitats and facilitating establishment beyond current ranges (Hellmann et al. 2008; Hulme 2017).

Among the two species, *S. kraussiana* appears likely to pose the greater future invasion risk. Total suitable habitat is projected to increase from 11.47 × $10^6$ km² under current conditions to 16.43 × $10^6$ km² under RCP 8.5 by 2080, representing a net gain of 4.96 × $10^6$ km² or approximately 43.2% relative to the current distribution (Table 4). Habitat expansion is concentrated in temperate and subtropical regions of East Asia, including eastern China, the Korean Peninsula, and southern Japan. Because the species can form dense mats that suppress native ground vegetation, these newly suitable areas may become increasingly susceptible to invasion (Nessia et al. 2014). Although climatic suitability is projected to decline in some tropical lowland regions under severe warming, many montane and subtropical areas are expected to remain suitable and may function as refugia and potential sources for further spread.

In contrast, *S. uncinata* exhibited only minor changes in suitable habitat, with total suitable area increasing from 2.95 × $10^6$ km² under current conditions to 3.04 × $10^6$ km² under RCP 8.5 in 2080, representing a net gain of only 0.09 × $10^6$ km², equivalent to approximately 3.1% of the current suitable habitat area (Table 4). Suitable habitats in southern China, Taiwan, and other humid subtropical regions remained largely persistent, reflecting the species' strong association with precipitation and stable humid environments. Consequently, future invasion risk is more likely to involve local persistence and gradual spread within climatically suitable habitats rather than broad geographic expansion.

These projections provide a basis for regional management prioritization. Surveillance efforts for *S. kraussiana* should focus on emerging suitable habitats in East Asia, whereas monitoring of *S. uncinata* should target humid montane and subtropical environments. Key management priorities include preventing ornamental releases, improving early detection, and implementing rapid responses to newly established populations before widespread naturalization occurs (Hulme 2017).

*Comparison with previous studies*

The present findings are broadly consistent with previous *Selaginella* distribution studies in Asia. Setyawan et al. (2018) identified temperature seasonality (bio_4) and dry-season precipitation as important predictors for *Selaginella ciliaris* and *S. plana* in Southeast Asia, supporting the importance of climatic seasonality and moisture-related variables observed in the present study. Likewise, Setyawan et al. (2021) projected future range expansion for *Selaginella zollingeriana* under climate-change scenarios, a pattern comparable to the substantial habitat expansion projected for *S. kraussiana*. However, the comparatively stable distribution pattern of *S. uncinata*, despite belonging to the same genus, indicates that closely related species may exhibit markedly different responses to future climate change due to differences in ecological requirements and climatic constraints (Pearman et al. 2010).

The projected expansion of *S. kraussiana* into higher-latitude and higher-elevation regions is also consistent with patterns reported for several invasive ferns and herbaceous invaders under future warming scenarios. Studies on *Lygodium microphyllum*, *Mikania micrantha*, and *Chromolaena odorata* similarly reported poleward or upslope expansion associated with increasing temperatures and changing climatic suitability (Volin et al. 2004; Banerjee et al. 2019; le Roux et al. 2019). In contrast, the relatively limited changes projected for *S. uncinata* suggest greater climatic stability and stronger dependence on persistently humid habitats. Unlike many invasive ferns that are strongly associated with disturbed habitats, both *Selaginella* species examined here may persist within shaded and humid understory environments, potentially increasing ecological persistence following establishment (Nessia et al. 2014).

Methodologically, the present study follows widely recommended species-distribution modeling practices through the application of spatial thinning, cross-validation, and multiple future climate scenarios (Kramer-Schadt et al. 2016; Phillips et al. 2017). The analysis further incorporated projections across four RCP scenarios (2.6, 4.5, 6.0, and 8.5) and three future periods (2030, 2050, and 2080), allowing evaluation of both short- and long-term responses to climate change. One notable aspect of this study is the inclusion of UVB-related variables in addition to standard bioclimatic predictors. The increasing contribution of UVB seasonality and UVB intensity variables under several future scenarios, particularly for *S. kraussiana*, suggests that radiation-related factors may influence habitat suitability under changing climates. Because most previous SDM studies have relied primarily on temperature and precipitation variables (Fick and Hijmans 2017), the present results indicate that incorporating UVB-related predictors may provide additional ecological insight into the environmental factors shaping the distribution of some *Selaginella* species.

## Integrating field observations and socio-ecological context: A more complete picture of invasion risk

The MaxEnt projections indicate that large parts of East, South, and Southeast Asia are climatically suitable for both *S. kraussiana* and *S. uncinata*, with *S. kraussiana* projected to expand substantially under future climate scenarios. However, long-term field observations suggest that climatic suitability alone does not fully explain realized invasion outcomes. Evidence supporting this interpretation includes RAPFISH-based sustainability assessment (Pitcher and Preikshot 2001) of *S. kraussiana* cultivation systems in Central Java, Indonesia (Setyawan et al. 2025), long-term observations of *S. uncinata* naturalization in Java between 2011 and 2025, and observations of spontaneous spore germination in native *Selaginella* species in Karanganyar, Central Java. Earlier studies also documented wild populations of *S. uncinata* in Cibodas Botanical Garden

(West Java) and Wonosobo (Central Java) outside intentional cultivation (Setyawan 2014).

### *The naturalization paradox: Contrasting outcomes of two introduced* Selaginella *species in Java*

A notable contrast emerges between predicted climatic suitability and realized naturalization patterns of the two introduced species. Although *S. kraussiana* is widely cultivated as an ornamental ground-cover plant and large parts of Java appear climatically suitable, persistent wild populations have not been documented outside managed cultivation sites. Field observations and RAPFISH analysis indicate that cultivation systems remain strongly dependent on managed microhabitats and informal ornamental trade networks (Setyawan et al. 2025). Even within forests, riparian zones, and abandoned agricultural lands, spontaneous establishment has not been observed. Current cultivation practices also rely predominantly on vegetative propagation rather than spore-based reproduction, potentially limiting natural dispersal capacity.

In contrast, *S. uncinata* has established self-sustaining wild populations despite comparatively lower climatic suitability predicted by the MaxEnt model. Earlier observations documented naturalized populations in Wonosobo and Cibodas Botanical Garden, where the species spread into stream margins, forest edges, greenhouse floors, and other shaded, disturbed habitats (Setyawan 2014). Previous transplant observations further indicated that *S. uncinata* can reproduce across different elevations and spread rapidly through vegetative growth, occasionally forming dense mats that compete with native creeping *Selaginella* species.

Additional observations from Karanganyar further support the importance of reproductive biology in explaining these contrasting outcomes. Following herbarium collection activities, spontaneous germination of several native *Selaginella* species, including *S. ciliaris*, *S. plana*, and *S. repanda*, was observed after rainy periods. These observations indicate that environmental conditions in Java are generally suitable for spore germination in some *Selaginella* species. However, despite repeated observations in ornamental cultivation sites, spontaneous establishment of *S. kraussiana* outside managed containers has not been detected.

### *Explaining the paradox: Factors potentially limiting* S. kraussiana *naturalization*

Taken together, these observations suggest that the limited naturalization of *S. kraussiana* in Java may not primarily reflect macroclimatic unsuitability, but rather constraints operating at reproductive and microsite levels. The species may produce fewer viable spores under Javan conditions, require specific establishment sites, or exhibit lower tolerance to local biotic interactions than other *Selaginella* species. Its dependence on vegetative propagation may also restrict long-distance dispersal and spontaneous colonization outside cultivation sites. RAPFISH analysis similarly indicated that current cultivation systems remain environmentally dependent and weakly integrated institutionally (Setyawan et al. 2025).

Conversely, the successful naturalization of *S. uncinata* suggests that the species possesses ecological traits favoring establishment after introduction, including broader tolerance of shaded moist habitats and effective vegetative spread. Earlier observations showed that the species can persist in forest margins, shaded riverbanks, stone walls, and other disturbed habitats while competing successfully with native ground-cover vegetation (Setyawan 2014). Rapid spread through vegetative fragmentation and rhizophore production may further facilitate local expansion under favorable environmental conditions.

### *Synthesis and implications for invasion risk assessment*

The combined evidence from species distribution modeling, field observations, and socio-ecological analysis demonstrates that climatic suitability alone is insufficient to determine invasion success. Although Java appears climatically suitable for both species, the current non-invasive status of *S. kraussiana* may be maintained by limited natural dispersal, dependence on human-assisted propagation, and specific establishment requirements that are not consistently met in natural ecosystems. The RAPFISH assessment additionally indicates that current cultivation systems remain environmentally dependent and may constrain broader landscape-scale spread despite favorable climatic suitability (Setyawan et al. 2025).

Long-term observations indicate that *S. uncinata* possesses several traits commonly associated with naturalized ornamental plants, including persistence in disturbed shaded habitats, rapid vegetative spread, and tolerance of humid environments (Setyawan 2014). These findings highlight the importance of integrating reproductive biology, long-term field observations, and socio-ecological context into invasion risk assessment. Reliance solely on climate-based species distribution models may overestimate invasion risk for species lacking effective natural reproduction or dispersal mechanisms. Nevertheless, future changes in climate, ornamental trade networks, and horticultural practices may alter current constraints and potentially increase opportunities for naturalization and spread.

## Limitations

This study has several limitations that should be considered when interpreting the results. The MaxEnt models were developed primarily from environmental predictors and therefore represent potential climatic suitability rather than realized species distributions. Important factors such as biotic interactions, dispersal barriers, propagule pressure, land-use change, habitat disturbance, and human-mediated introductions were not explicitly incorporated. In particular, ornamental trade networks and propagule pressure were not directly included in our models due to data limitations. Although occurrence records were cleaned and spatially thinned to reduce sampling bias, residual bias may remain because the data were compiled from multiple geographic regions and sources. Uncertainty associated with future climate projections, particularly precipitation forecasts, may also affect model predictions. In addition, the models assume climatic niche conservatism and do not account for evolutionary adaptation, phenotypic plasticity, or changes in species interactions under future environmental conditions. The contrasting naturalization patterns observed in Java further indicate that climate suitability alone may not fully determine invasion success. Future studies should integrate long-term field monitoring, demographic data, and socio-ecological factors to improve invasion-risk assessment and prediction accuracy. Therefore, the projected distributions should be interpreted as potential climatic suitability rather than realized future invasion outcomes.

In conclusion, climate change is projected to differentially affect the future distribution of two invasive *Selaginella* species across East, South, and Southeast Asia. The MaxEnt models showed excellent predictive performance, with AUC values of 0.935 and 0.966 for *S. kraussiana* and *S. uncinata*, respectively, and revealed distinct environmental controls on habitat suitability. *Selaginella kraussiana* was primarily associated with temperature-related variables, particularly the minimum temperature of the coldest month (bio_6), and is projected to undergo substantial habitat expansion under future warming scenarios, with suitable habitat increasing from 11.47 × $10^6$ $km^2$ to 16.43 × $10^6$ $km^2$ (+43.2%) under RCP 8.5 by 2080. Expansion is projected mainly into higher-latitude and higher-elevation subtropical and temperate regions. In contrast, *S. uncinata* was more strongly associated with annual precipitation (bio_12) and exhibited comparatively stable habitat suitability across future climate scenarios, with suitable habitat increasing only from 2.95 × $10^6$ $km^2$ to 3.04 × $10^6$ $km^2$ (+3.1%) under the same scenario. These findings indicate that *S. kraussiana* may pose a greater future climate-driven invasion risk, whereas *S. uncinata* is more likely to persist and spread gradually within existing humid subtropical and montane habitats. The study also demonstrates that climatic suitability alone may not fully explain invasion outcomes, highlighting the value of integrating species distribution modeling with field observations and socio-ecological evidence to improve invasion-risk assessment and climate-adaptive management of invasive lycophytes in Asia.

## ACKNOWLEDGEMENTS

The authors thank the Global Biodiversity Information Facility (GBIF) for providing open-access species occurrence data, WorldClim for climate data, the International Soil Reference and Information Center (ISRIC) for soil data, and the gIUV project for UVB radiation data. We acknowledge the Center for International Tropical Agriculture (CIAT) and the Program on Climate Change, Agriculture and Food Security (CCAFS) for future climate scenario data. This research received no specific grant from any funding agency in the public, commercial, or not-for-profit sectors. We declare no competing interests.

## REFERENCES

Aiello-Lammens ME, Boria RA, Radosavljevic A, Vilela B, Anderson RP. 2015. spThin: An R package for spatial thinning of species occurrence records for use in ecological niche models. Ecography 38 (5): 541-545. https://doi.org/10.1111/ecog.01132.

Allouche O, Tsoar A, Kadmon R. 2006. Assessing the accuracy of species distribution models: Prevalence, kappa and the True Skill Statistic (TSS). J Appl Ecol 43 (6): 1223-1232. https://doi.org/10.1111/j.1365-2664.2006.01214.x.

Banerjee AK, Mukherjee A, Dewanji A. 2019. Predicting the distribution of *Mikania micrantha* Kunth in Asia under climate change. Ecol Inform 52: 78-87.

Beckmann M, Václavík T, Manceur AM, Šprtová L, von Wehrden H, Welk E, Cord AF. 2014. glUV: A global UV-B radiation dataset for macroecological studies. Methods Ecol Evol 5 (4): 372-383. https://doi.org/10.1111/2041-210X.12168.

Bellard C, Bertelsmeier C, Leadley P, Thuiller W, Courchamp F. 2012. Impacts of climate change on the future of biodiversity. Ecol Lett 15 (4): 365-377. https://doi.org/10.1111/j.1461-0248.2011.01736.x.

Brownsey PJ, Perrie LR. 2018. Selaginellaceae. In: Breitwieser I, Wilton AD (eds.). Flora of New Zealand - Ferns and Lycophytes (Fascicle 21). Manaaki Whenua Press, New Zealand.

Dang ZPA, McLenachan PJ, Lockhart N, Waipara O, Reynolds C, Blanchon D. 2019. Metagenome profiling identifies potential biocontrol agents for *Selaginella kraussiana* in New Zealand. Genes 10 (2): 106. https://doi.org/10.3390/genes10020106.

Dormann CF, Elith J, Bacher S, Buchmann C, Carl G, Carré G, Lautenbach S. 2013. Collinearity: A review of methods to deal with it and a simulation study evaluating their performance. Ecography 36 (1): 27-46. https://doi.org/10.1111/j.1600-0587.2012.07348.x.

Elith J, Leathwick JR. 2009. Species distribution models: Ecological explanation and prediction across space and time. Annu Rev Ecol Evol Syst 40: 677-697. https://doi.org/10.1146/annurev.ecolsys.110308.120159.

Elith J, Phillips SJ, Hastie T, Dudík M, Chee YE, Yates CJ. 2011. A statistical explanation of MaxEnt for ecologists. Divers Distrib 17 (1): 43-57. https://doi.org/10.1111/j.1472-4642.2010.00725.x.

Farr TG, Rosen PA, Caro E, Crippen R, Duren R, Hensley S, Alsdorf D. 2007. The shuttle radar topography mission. Rev Geophys 45 (2): RG2004. https://doi.org/10.1029/2005RG000183.

Fick SE, Hijmans RJ. 2017. WorldClim 2: New 1 km spatial resolution climate surfaces for global land areas. Intl J Climatol 37 (12): 4302-4315. https://doi.org/10.1002/joc.5086.

GBIF. 2024. GBIF occurrence download. Global Biodiversity Information Facility. Available from: https://www.gbif.org.

Gola EM, Jernstedt JA. 2016. Vascular structure contributes to shoot sectoriality in *Selaginella kraussiana*. Acta Soc Bot Pol 85 (3): 3515. http://dx.doi.org/10.5586/asbp.3515.

Gorunescu F. 2011. Data Mining: Concepts and Techniques. Springer, Berlin. https://doi.org/10.1007/978-3-642-19721-5.

Hellmann JJ, Byers JE, Bierwagen BG, Dukes JS. 2008. Five potential consequences of climate change for invasive species. Conserv Biol 22 (3): 534-543. https://doi.org/10.1111/j.1523-1739.2008.00951.x.

Hengl T, Mendes de Jesus J, Heuvelink GBM, Ruiperez Gonzalez M, Kilibarda M, Blagotić A, Kempen B. 2017. SoilGrids250m: Global gridded soil information based on machine learning. PLoS ONE 12 (2): e0169748. https://doi.org/10.1371/journal.pone.0169748.

Hughes AC. 2017. Understanding the drivers of Southeast Asian biodiversity loss. Ecosphere 8 (1): e01624. https://doi.org/10.1002/ecs2.1624.

Hulme PE. 2009. Trade, transport and trouble: Managing invasive species pathways in an era of globalization. J Appl Ecol 46 (1): 10-18. https://doi.org/10.1111/j.1365-2664.2011.02069.x.

Hulme PE. 2017. Climate change and biological invasions: Evidence, expectations, and response options. Biol Rev 92 (3): 1297-1313. https://doi.org/10.1111/brv.12282.

IPCC. 2021. Climate Change 2021: The Physical Science Basis. Contribution of Working Group I to the Sixth Assessment Report of the Intergovernmental Panel on Climate Change. Cambridge University Press, Cambridge.

Khairunnisa H, Dewi MAK, Faqiih MAH, Putrayuda MR, Nugroho GD, Indrawan M, Setyawan AD. 2024. Prediction of potential climate change impacts on the geographic distribution shift of *Casuarina junghuhniana* and *C. equisetifolia* in Southeast Asia. Biodiversitas 23: 6360-6371.

Kramer-Schadt S, Niedballa J, Pilgrim JD, Schröder B, Lindenborn J, Reinfelder V, Wilting A. 2016. The importance of correcting for sampling bias in MaxEnt species distribution models. Divers Distrib 19 (11): 1366-1379. https://doi.org/10.1111/ddi.12096.

le Roux JJ, Hui C, Keletso M, Richardson DM. 2019. Recent range expansion of *Chromolaena odorata* in Africa: A climate change signal? Biol Invasions 21 (8): 2657-2670.

Li L, Yang L, Qin A, Jiang F, Chen L, Deng R. 2022. Anatomical and biochemical traits related to blue leaf coloration of *Selaginella uncinata*. J Healthc Eng 2022: 1005449. https://doi.org/10.1155/2022/1005449.

Li R, Xu M, Wong MHG, Qiu S, Li Q, Liu Y. 2021. Climate change threatens the distribution of major Himalayan plant species. Glob Ecol Conserv 27: e01575.

Myers N, Mittermeier RA, Mittermeier CG, da Fonseca GAB, Kent J. 2000. Biodiversity hotspots for conservation priorities. Nature 403 (6772): 853-858. https://doi.org/10.1038/35002501.

Navarro-Racines C, Tarapues J, Thornton P, Jarvis A, Ramírez-Villegas J. 2020. High-resolution and bias-corrected CMIP5 projections for climate change impact assessments. Sci Data 7 (1): 7. https://doi.org/10.1038/s41597-019-0343-8.

Nessia HR, Dale AR, Perrott JK, Waipara NW, Aguilar GD, Blanchon DJ. 2014. Comparison of species richness and frequency cover of forest floor plants and lichens in sites invaded and uninvaded by the invasive club moss *Selaginella kraussiana* (Kunze) A. Braun. Plant Prot Q 29 (2): 66-70.

Parmesan C, Yohe G. 2003. A globally coherent fingerprint of climate change impacts across natural systems. Nature 421 (6918): 37-42. https://doi.org/10.1038/nature01286.

Pearman PB, D'Amen M, Graham CH, Thuiller W, Zimmermann NE. 2010. Within-taxon niche structure: Niche conservatism, divergence and predicted effects of climate change. Ecography 33 (6): 990-1003. https://doi.org/10.1111/j.1600-0587.2010.06443.x.

Phillips SJ, Anderson RP, Dudík M, Schapire RE, Blair ME. 2017. Opening the black box: An open-source release of Maxent. Ecography 40 (7): 887-893. https://doi.org/10.1111/ecog.03049.

Phillips SJ, Anderson RP, Schapire RE. 2006. Maximum entropy modeling of species geographic distributions. Ecol Model 190 (3-4): 231-259. https://doi.org/10.1016/j.ecolmodel.2005.03.026.

Phillips SJ, Dudík M. 2008. Modeling of species distributions with Maxent: New extensions and a comprehensive evaluation. Ecography 31 (2): 161-175. https://doi.org/10.1111/j.0906-7590.2008.5203.x.

Pyšek P, Hulme PE, Simberloff D, Bacher S, Blackburn TM, Carlton JT, Richardson DM. 2020. Scientists' warning on invasive alien species. Biol Rev 95 (6): 1511-1534. https://doi.org/10.1111/brv.12627.

Qin G, Lei J, Li S, Jiang Y, Qiao L, Ren M, Gao X. 2022. Efficient, green extraction of two biflavonoids from *Selaginella uncinata* with deep eutectic solvents. Microchem J 183: 108085. https://doi.org/10.1016/j.microc.2022.108085.

Pitcher TJ, Preikshot D. 2001. RAPFISH: A rapid appraisal technique to evaluate the sustainability status of fisheries. Fish Res 49 (3): 255-270. https://doi.org/10.1016/S0165-7836(00)00205-8.

R Core Team. 2022. R: A Language and Environment for Statistical Computing. R Foundation for Statistical Computing, Vienna. Available from: https://www.R-project.org/

Setyawan AD, Sugiyarto, Susilowati A, Widodo. 2015. Diversity and distribution of *Selaginella* in the province of Yogyakarta Special Region. Pros Sem Nas Masy Biodiv Indon 1 (5): 987-992. https://doi.org/10.13057/psnmbi/m010505.

Setyawan AD, Supriatna J, Nisyawati N, Nursamsi I, Sutarno S, Sugiyarto S, Pradhan P. 2021. Projecting the expansion range of *Selaginella zollingeriana* in the Indonesian archipelago under future climate conditions. Biodiversitas 22 (4): 2088-2103. https://doi.org/10.13057/biodiv/d220458.

Setyawan AD, Supriatna J, Nisyawati N, Sutarno S, Nursamsi I. 2018. Predicting impacts of future climate change on the distribution of the widespread selaginellas (*Selaginella ciliaris* and *S. plana*) in Southeast Asia. Biodiversitas 19 (5): 1960-1977. https://doi.org/10.13057/biodiv/d190548.

Setyawan AD, Sutarno, Sugiyarto, Sunarto, Dianti. 2025. Sustainability transitions and invasive risk in the trade and cultivation of *Selaginella kraussiana* in tropical Indonesia. Asian J Agric 9 (2): 925-940. https://doi.org/10.13057/asianjagric/g090258.

Setyawan AD. 2011. Recent status of *Selaginella* (Selaginellaceae) research in Nusantara. Biodiversitas 12 (2): 112-124. https://doi.org/10.13057/biodiv/d120209.

Setyawan AD. 2014. A new record of naturalized *Selaginella uncinata* (Desv.) Spring (Selaginellaceae) from Java, Indonesia. Biodiversitas 15 (2): 261-268. https://doi.org/10.13057/biodiv/d150221.

Sodhi NS, Koh LP, Brook BW, Ng PKL. 2004. Southeast Asian biodiversity: An impending disaster. Trends Ecol Evol 19 (12): 654-660. https://doi.org/10.1016/j.tree.2004.09.006.

Volin JC, Lott MS, Muss JD, Owen D. 2004. Predicting rapid invasion of the Florida Everglades by *Lygodium microphyllum*. Wetlands 24 (4): 928-938.

Warren DL, Seifert SN. 2011. Ecological niche modeling in Maxent: The importance of model complexity and the performance of model selection criteria. Ecol Appl 21 (2): 335-342. https://doi.org/10.1890/10-1171.1.

Wei T, Simko V. 2021. R package 'corrplot': Visualization of a correlation matrix (Version 0.92). Available from: https://github.com/taiyun/corrplot.

West AM, Kumar S, Brown CS, Stohlgren TJ, Bromberg J. 2016. Field validation of an invasive species Maxent model. Ecol Inform 36: 126-134. https://doi.org/10.1016/j.ecoinf.2016.11.001.